ACS ENVIRONMENTAL Au
AN OPEN ACCESS JOURNAL OF THE AMERICAN CHEMICAL SOCIETY

pubs.acs.org/environau
Article

Advancing Microbial Electrochemical H_2O_2 Synthesis by Tailoring the Surface Chemistry of Stereolithography-Derived 3D Pyrolytic Carbon Electrodes

Published as part of ACS Environmental Au special issue "2024 Rising Stars in Environmental Research".

Rusen Zou,[§] Babak Rezaei,[§] Stephan Sylvest Keller, and Yifeng Zhang*

Cite This: ACS Environ. Au 2024, 4, 344−353
Read Online

ACCESS | Metrics & More | Article Recommendations | Supporting Information

ABSTRACT: Microbial electrosynthesis of H_2O_2 offers an economical and eco-friendly alternative to the costly and environmentally detrimental anthraquinone process. Three-dimensional (3D) electrodes fabricated through additive manufacturing demonstrate significant advantages over carbon electrodes with two-dimensional (2D) surfaces in microbial electrosynthesis of H_2O_2. Nevertheless, the presence of oxygen-containing free acidic groups on the prototype electrode surface imparts hydrophilic properties to the electrode, which affects the efficiency of the two-electron oxygen reduction reaction for H_2O_2 generation. In this study, we elucidated that the efficiency of microbial H_2O_2 synthesis is markedly enhanced by utilizing oxygen-free 3D electrodes produced via additive manufacturing techniques followed by surface modifications to eradicate oxygen-containing functional groups. These oxygen-free 3D electrodes exhibit superior hydrophobicity compared to traditional carbon electrodes with 2D surfaces and their 3D printed analogues. The oxygen-free 3D electrode is capable of generating up to 130.2 mg L^{-1} of H_2O_2 within a 6-h time frame, which is 2.4 to 13.6 times more effective than conventional electrodes (such as graphite plates) and pristine 3D printed electrodes. Additionally, the reusability of the oxygen-free 3D electrode underscores its practical viability for large-scale applications. Furthermore, this investigation explored the role of the oxygen-free 3D electrode in the bioelectro-Fenton process, affirming its efficacy as a tertiary treatment technology for the elimination of micropollutants. This dual functionality accentuates the versatility of the oxygen-free 3D electrode in facilitating both the synthesis of valuable chemicals and advancing environmental remediation. This research introduces an innovative electrode design that fosters efficient and sustainable H_2O_2 synthesis while concurrently enabling subsequent environmental restoration.

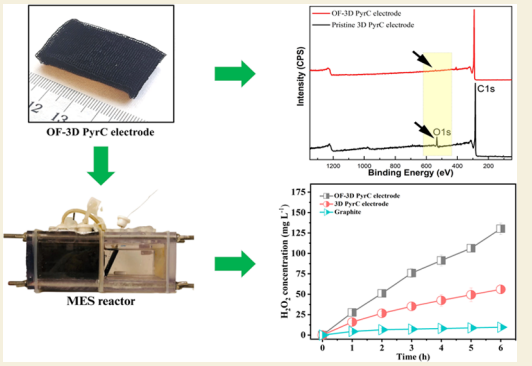

KEYWORDS: *additive manufacturing, surface modification, H_2O_2, oxygen-free, microbial electrosynthesis*

1. INTRODUCTION

Hydrogen peroxide (H_2O_2) is a crucial chemical in various industries. In 2020, its production reached 4.5 million metric tons and it is expected to continue growing.[1] H_2O_2 is widely used in pulp and paper bleaching, chemical synthesis, and wastewater treatment.[2] However, the current production methods, mainly via anthraquinone oxidation, are both costly (around 100 EUR per ton) and energy-intensive, generating significant waste.[3,4] Additionally, H_2O_2 is hazardous to transport and store, making in situ synthesis favorable for many applications.[5]

One promising method for in situ production is electrolysis, which is cost-efficient and mitigates storage and transport risks.[5] H_2O_2 is produced from the oxygen reduction reaction (ORR) with a two-electron transfer (eq 1).[6,7] A critical factor in the electrochemical synthesis of H_2O_2 is the electrode's selectivity toward the two-electron ORR, as the four-electron ORR simply produces water (eq 2).[6,8] Additionally, the formed H_2O_2 can further be reduced to water (eq 3).[6] The electrode surface area is also essential to ensure numerous active sites for H_2O_2 synthesis.[9] However, high electrode costs can hinder large-scale commercial and industrial processes.[2] Carbon materials are promising as electrodes due to their abundance, low cost, and transportability.[8] Despite its potential, the electrochemical synthesis of H_2O_2 still has high energy requirements.[10]

$$O_2 + 2H^+ + 2e^- \rightarrow H_2O_2 \quad (1)$$

Received: July 30, 2024
Revised: October 1, 2024
Accepted: October 2, 2024
Published: October 15, 2024

$$O_2 + 4H^+ + 4e^- \rightarrow 2H_2O \quad (2)$$

$$H_2O_2 + 2H^+ + 2e^- \rightarrow 2H_2O \quad (3)$$

Recently, microbial electrochemical technologies (METs) have gained interest as a less energy-intensive alternative for H_2O_2 synthesis.[11] METs leverage electrochemical reactions between microbes and an electrode, with part of the required energy being green and harvested from wastewater.[12] Specifically, organic matter in wastewater is degraded by electroactive bacteria (typically Geobacter spp.) adhering to the surface of the carbon fiber electrode serving as anode, yielding electrons, protons, and CO_2 (eq 4).[13] H_2O_2 synthesis at the cathode of METs is possible with or without an external power supply, but an added power supply on top of the one delivered by the bioanode significantly increases the final H_2O_2 concentration in the cathodic chamber, even with low voltage (<1 V).[11,14] The characteristics of the cathode are vital for H_2O_2 generation through microbial electrochemical synthesis. Therefore, it essential to develop energy-efficient catalysts with a high rate of H_2O_2 production. Generally, precious-metal-free carbon electrodes are preferred for the cathode, as precious-metal-based electrodes can favor the four-electron ORR (eq 3).[15] The cathode electrode should have good mechanical stability, electrical conductivity, high surface area, and relatively low costs.[14] Among the diverse cathode materials, carbon-based materials have garnered significant interest due to their high tunability and eco-friendliness. Recently, carbon-based materials, including conventional graphite electrodes with two-dimensional (2D) surface and additive manufacturing-derived free-standing three-dimensional pyrolytic carbon (3D PyrC) electrodes with 3D geometries, have been utilized as cathode materials for H_2O_2 production.[13,16] The integration of high-resolution lithography-based 3D printing followed by a carbonization process has emerged as a new approach for fabricating free-standing, complex 3D carbon geometries with greater design flexibility and scalability compared to conventional structural engineering and microfabrication techniques.[17−19] These advanced materials have been utilized in a diverse range of applications, from electrical energy storage (EES) devices to power-to-chemistry systems.[13,20] The elevated H_2O_2 yield and current efficiency of the 3D PyrC electrode compared to conventional carbon electrodes (e.g., graphite) suggest that this material possesses significant potential for energy-efficient H_2O_2 synthesis.[17]

$$C_aH_bO_c + (2a - c)H_2O \rightarrow aCO_2 + (b + 4a - 2c)H^+ + (b + 4a - 2c)e^- \quad (4)$$

However, research has revealed that the surface of prototype 3D PyrC electrodes contains a significant number of oxygen-containing acidic groups (−COOH, −COH, −COO−), which render the electrode surface hydrophilic.[21] This hydrophilicity may reduce the adsorption and reactivity of oxygen at the interface, thereby inhibiting the efficiency of the two-electron ORR.[9] While 3D PyrC materials hold immense promise for a wide range of applications, tailoring their surface chemistry remains a largely untapped area, inviting for further exploration and innovation. The performance of H_2O_2 generation, closely linked to the electronic structure of the electrode, can be enhanced by inducing charge redistribution, which tunes the electronic structure of carbon materials to create more active sites for two-electron ORR.[9] Accordingly, electrode surface modification has been proposed to enhance the H_2O_2 selectivity of electrodes.[6] A wide range of dopants have been investigated for electrode modification to enhance the electrochemical synthesis of H_2O_2, but no research has focused on oxygen-free cathode electrodes.[5,22]

In this study, we developed and implemented an innovative, cost-effective, rapid, and straightforward approach to fabricate oxygen-free 3D pyrolytic carbon (OF-3D PyrC) electrodes for H_2O_2 production in microbial electrochemical systems (MES). This method integrates high-resolution stereolithography (SLA) 3D printing, surface modification of the 3D printed polymer precursor, and a subsequent pyrolysis process. The effectiveness of the OF-3D PyrC electrode for in situ H_2O_2 synthesis was extensively evaluated across various parameters, including cathodic electrolyte pH, input voltage, cathodic aeration rate, and supporting electrolyte. Beyond assessing the novel OF-3D PyrC electrode for H_2O_2 synthesis, this study further evaluates its potential in the bioelectro-Fenton (BEF) process as a tertiary treatment technology, aiming to effectively remove recalcitrant micropollutants from WWTP secondary effluent. Consequently, the 24 pharmaceuticals investigated for removal are among the most frequently detected micropollutants in the secondary effluent of EU WWTPs. The findings offer new perspectives on developing an innovative, cost-efficient, and energy-saving technology for H_2O_2 production with concurrent wastewater treatment.

2. MATERIALS AND METHODS

2.1. Preparation of 3D Pyrolytic Carbon Electrodes

A novel and simple approach was developed for the first time for the fabrication of less hydrophilic (oxygen-free surface) free-standing 3D carbon electrodes to significantly enhance selective H_2O_2 synthesis in MES. The less hydrophilic surface improves bubble entrapment within the structure, leading to more air-saturated surfaces and thereby boosting the two-electron ORR kinetics. For this purpose, a 3D reticular polymer structure (cubic mesh structure with approximately 74 mm length, 43 mm width, and 12.4 mm height) was designed using Fusion 360 software (Education License, V. 2.0.13881, Autodesk, Inc.). The reticular design was chosen for this research to potentially improve mass transport within the electrode, achieve better printability compared to more complex geometries, and attain high reproducibility with the 3D printing technique. However, the potential of the employed approach to fabricate 3D carbon electrodes with various geometries has been demonstrated in other research.[20,23] The dimensions of the reticular design were determined in preliminary experiments to reach the minimum printable dimensions of the crossbar, achieve higher degassing surfaces, preserve the structure during the pyrolysis process and prevent bulging and deformation through thermal treatment. Moreover, since it was assumed that a more open design could help for better mass transport, the main goal was finding the optimum open unit sizes so that structure would not collapse after 3D printing and during the pyrolysis process. After some preliminarily experiments, the optimal design was chosen as the reticular pattern with a unit size of 1.5 mm and circular crossbars with a 350 μm diameter. The stereolithography file (.stl) was introduced into slicing software (Preform V. 3.38.0 Formlabs Inc.) to prepare a stereolithography 3D printing code. The 3D reticular polymer architecture was printed using a Formlabs 2 stereolithography (SLA) 3D printer (Formlabs Inc.) with a commercial photopolymer (Formlabs high-temperature resin, HTR) employed as the precursor material. HTR resin, composed of acrylated monomers and methacrylated oligomers, was selected for this research due to its proven potential to preserve shape and features during the pyrolysis process, as demonstrated in previous studies.[17,24] Following the 3D printing, the printed structures were removed from the build platform, washed with isopropanol for a few minutes, and

https://doi.org/10.1021/acsenvironau.4c00067
ACS Environ. Au 2024, 4, 344−353

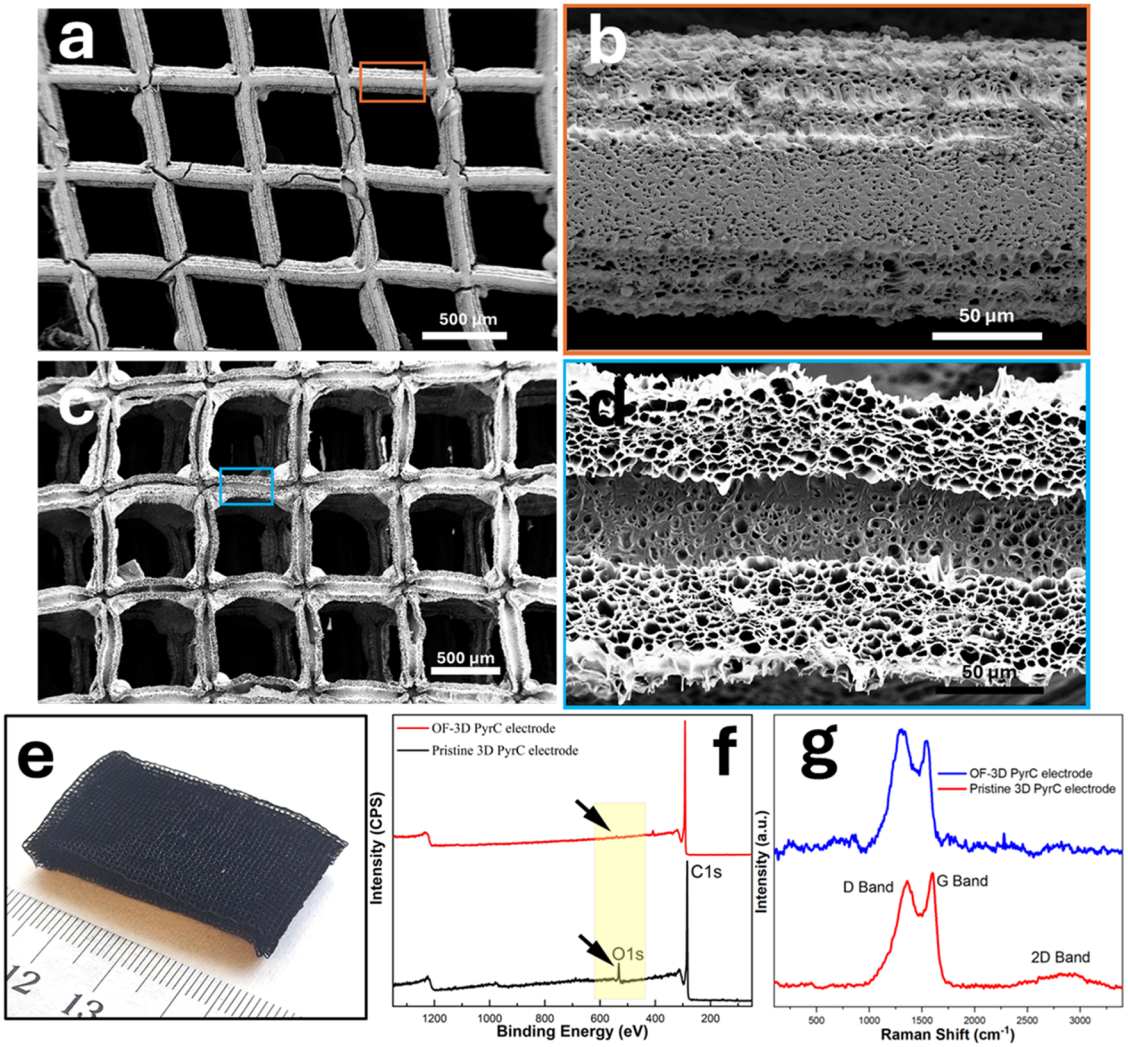

Figure 1. SEM images of (a, b) the pristine and (c, d) OF-3D PyrC electrode, (e) A photograph of the OF-3D PyrC electrode, (f) XPS survey spectra and (g) Raman spectra of the pristine and OF-3D PyrC electrode.

postcured in a UV exposure chamber for an additional 5 min. The 3D printed architecture was then spray-coated with 10 mL of a 6 wt % polytetrafluoroethylene (PTFE) dispersion in water and dried in an oven at 80 °C overnight. Afterward, the sample was carbonized gradually using a ceramic tube furnace (MTI Corp., GSL 1700x) at 1000 °C under flowing N_2 to produce OF-3D PyrC electrodes. The gradual pyrolysis process was designed based on the onset and maximum decomposition temperatures of the cured HT resin employed in this research. Briefly, the gradual pyrolysis process involved the following steps: heating at 2 °C min^{-1} up to 375 °C, holding at this temperature for 90 min, then heating at 1 °C min^{-1} to 425 °C and maintaining it for another 90 min, and finally heating at 3 to 1000 °C, where it was held for 60 min. The furnace was then cooled to room temperature under flowing N_2. A detailed pyrolysis profile can be found in our previous research.[13] To fabricate pristine 3D PyrC electrodes, the same process was followed, except the spray-coating with PTFE dispersion was not applied. Finally, the electrodes were sewn with a piece of titanium wire (0.1 mm in diameter) and employed as the cathode in a MES reactor.

2.2. Physicochemical Characterization

The shape, morphology and surface topography of the pristine and OF-3D PyrC electrodes were characterized using a scanning electron microscope (SEM, Zeiss Supra VP 40, Germany). X-ray photoelectron spectroscopy (XPS, Thermo Scientific Nexsa) was utilized to assess the elemental composition, chemical state and surface functionality of the pristine and OF-3D PyrC electrodes. Raman spectroscopy was performed using a Thermo Scientific Nexsa micro-Raman system with a 532 nm laser wavelength.

2.3. MES Reactor Configuration and Operation

A dual-chamber (400 mL total volume) MES reactor constructed from polycarbonate was developed (Figure S1). The two compartments (8 cm in length, 5 cm in width, and 5 cm in height) were divided by a cation exchange membrane (CMI 7001, Membrane International, NJ). The anode chamber utilized a commercially available carbon brush (5.9 cm in diameter, 6.9 cm in length, Mill-Rose) with a high specific surface area, while the cathode employed a newly designed OF-3D PyrC electrode. It is important to note that both the commercial cation exchange membranes and carbon brushes mentioned above must be pretreated before reactor installation, as detailed in our previous research.[10] Following the assembly of the reactor, the initial step involved enriching the electrochemically active bacteria at the anode. The inoculum was sourced from the influent water of a wastewater treatment plant (WWTP) (Lundtofte, Copenhagen, Denmark), with an additional 1 g L^{-1} sodium acetate added to enrich the electrochemically active bacteria. The reactor operated in microbial fuel cell (MFC) mode during this period, with a 1000 Ω resistor connected in series between the anode and cathode. Additionally, a 50 mM potassium ferricyanide solution containing 50 mM phosphate buffer (pH 7.2) was used as the cathodic electrolyte. After one month of anodic enrichment, a mature biofilm formed, enabling the reactor to produce a stable and repeatable voltage of up to 0.72 V.

https://doi.org/10.1021/acsenvironau.4c00067
ACS Environ. Au 2024, 4, 344−353

The anode chamber was continuously supplied with WWTP influent wastewater, supplemented with 1 g L^{-1} sodium acetate. The anode was connected to a 500 mL recirculation bottle via a peristaltic pump, circulating the anode solution at 30 mL min^{-1}. The cathode chamber contained 180 mL of 50 mM sodium sulfate solution at pH 2, operating in batch mode. Various operational parameters, including input voltage, cathodic aeration rate, catholyte pH, and electrolyte type and concentration, were evaluated for their effect on the performance of the OF-3D PyrC electrodes for H_2O_2 synthesis. The OF-3D PyrC electrode was also tested in a BEF process for removing 24 typical pharmaceuticals (Sigma, Denmark) at concentrations ranging from 20 to 130 μg L^{-1} (see Text S1). Reactor settings were based on the H_2O_2 synthesis experiment, with a ferrous sulfate dosage of 0.2 mM.

2.4. Analytical Methods

A pH meter (PHM 210, Radiometer) measured sample pH, while a digital DO meter (Multi 3420, WTW, UK) with an optical IDS DO sensor (FDO 925, WTW, UK) assessed the dissolved oxygen (DO) of the catholyte. H_2O_2 concentration was determined spectrophotometrically (Spectronic 20D+, Thermo Scientific). Electrochemical studies used a 100 mL three-electrode setup with the 3D PyrC electrode as the working electrode, an Ag/AgCl in 3 M KCl as the reference, and a platinum wire coil as the counter electrode. These analyses were performed using an Autolab PGSTAT128N potentiostat/galvanostat with NOVA software, version 2.1.4 (Metrohm Autolab BV, The Netherlands). Linear sweep voltammetry (LSV) was run at 10 mV s^{-1}. A high-performance liquid chromatography system (Agilent 1290 Infinity) coupled with a tandem mass spectrometer (Agilent 6470 series, USA, MS/MS) quantified 24 typical pharmaceuticals, with operational details described in Text S2. System voltage was recorded every 30 min by a data acquisition system (Model 2700, Keithley Instruments, Inc., Cleveland, OH), and current was calculated using Ohm's law. Current efficiency and energy consumption for H_2O_2 synthesis were calculated as described in Text S3.

3. RESULTS AND DISCUSSION

3.1. Morphology and Material Properties of 3D PyrC Electrodes

In recent years, the integration of high-resolution lithography-based 3D printing followed by a carbonization process has emerged as a new approach for fabricating free-standing, complex 3D carbon electrode geometries with greater design flexibility and scalability compared to conventional structural engineering and microfabrication techniques.[17−19] These advanced materials have been utilized in a diverse range of applications, from electrical energy storage (EES) devices to power-to-chemistry systems.[13,20] However, tailoring and modifying the surface chemistry of these unique materials remains as underexplored area, with significant potential for further research and development. The primary hypothesis of this research was that tailoring the surface chemistry of 3D PyrC electrodes can significantly influence the performance of the two-electron ORR in MES. Specifically, creating a less hydrophilic carbon surface may facilitate improved bubble entrapment within the structure, leading to more air-saturated surfaces, which are crucial for boosting the efficiency of the 2$\bar{e}$ ORR and H_2O_2 electrosynthesis.

Therefore, in this research, a thin film coating of PTFE was employed to tailor the surface chemistry of the derived carbon electrodes, as PTFE is both pyrolysable and free of elements that could generate hydrophilic functional groups (e.g., nitrogen and oxygen). SEM images of the pristine and PTFE-modified 3D PyrC electrodes (Figure 1 a-d) reveal that while the reticular pattern is maintained throughout the high-temperature pyrolysis process, distinct differences in the surface topography are evident between the two samples. The differences are more pronounced in the higher magnification SEM images (Figure 1 b and d), which clearly demonstrate that the presence of a thin layer of PTFE on the 3D polymer precursor structures significantly enhances the surface topography of the derived 3D carbon microstructures, resulting in a rough and more porous surface. Figure 1e presents a photograph of the fabricated electrode, demonstrating the capability of the developed technique to produce electrodes with dimensions on the centimeter scale in the X and Y axes, and several millimeters in the Z axis. The three bigger rectangular holes visible in the center of the electrode were designed to facilitate the secure attachment of the titanium wire and improve the connection of the electrode within the MFC reactor. Figure 1f presents the XPS spectra of both the pristine and PTFE-modified 3D PyrC electrodes. The elemental analysis of the pristine 3D PyrC material reveals an oxygen content of approximately 6−7 atomic % on the surface. In contrast, the case of PTFE-modified 3D PyrC material exhibits no detectable oxygen, indicating the success of the employed technique in achieving a surface with no oxygen-based functional groups. Since the modified sample has been demonstrated to lack oxygen-based functional groups, it will hereafter be referred to as oxygen-free (OF)-3D PyrC electrodes throughout the paper. Figure 1g compares the Raman spectra of the pristine and OF-3D PyrC electrodes, highlighting the characteristic features of the two pyrolytic carbon materials. The spectra show the G band, associated with crystalline graphite, at around 1580 cm^{-1}, and the D band, indicative of amorphous carbon structure or various types of defects within the graphite domains, at around 1360 cm^{-1}. Moreover, the presence of a broad and diffuse 2D band at around 2700 cm^{-1} in the spectra indicates the existence of disordered and randomly arranged graphene structures within the materials. The size of the in-plan crystallite domains (Lα), indicative of the graphitic microcrystalline regions, is empirically estimated to be inversely related to the ratio of the intensities of the D and G bands (i.e., $L\alpha \propto 1/(I_D/I_G)$. The OF-3D PyrC sample exhibits a significantly higher I_D/I_G ratio (1.06) compared to the pristine 3D PyrC electrode (0.94). The higher I_D/I_G ratio value for modified sample indicates smaller in-plan crystalline domains, which may be interpreted as a reduced fraction of graphitic microdomains and/or an increase in disorder or defects within the OF-3D PyrC material.[25,26]

3.2. Microbial Electrosynthesis of H_2O_2 Using OF-3D PyrC Electrodes

First, the performance of the OF-3D PyrC electrode in H_2O_2 synthesis was compared with that of the pristine 3D PyrC electrode and the traditional graphite plate electrodes. The properties of these traditional electrodes have been extensively examined previously. Therefore, rather than duplicating the characterization, we referenced the pertinent literature.[13,27] Figure 2 illustrates the variation in H_2O_2 concentration within the MES reactor as a function of operating time with different cathode materials. Regardless of the electrode type employed, the concentration of H_2O_2 accumulated at the cathode increased linearly over time. The highest H_2O_2 concentration after 6 h was achieved with the novel OF-3D PyrC electrode, reaching 130.2 mg L^{-1}, followed by the pristine 3D PyrC electrode, gas diffusion electrode (GDE), carbon cloth and

https://doi.org/10.1021/acsenvironau.4c00067
ACS Environ. Au 2024, 4, 344−353

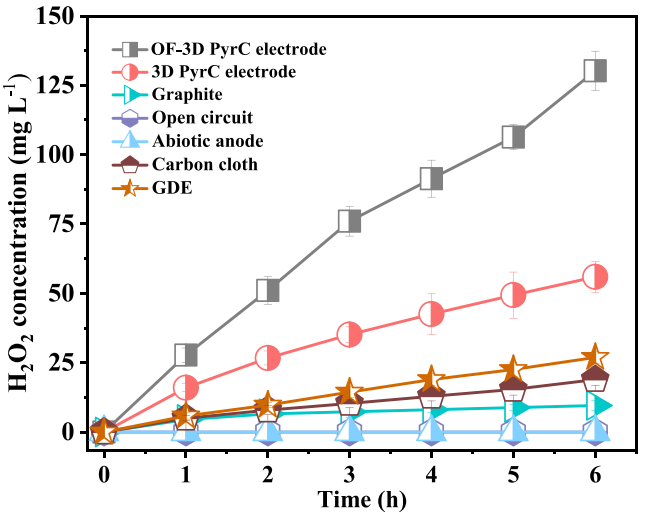

Figure 2. Microbial electrosynthesis of H_2O_2 using OF-3D PyrC electrode and comparison pristine 3D PyrC and different conventional carbon electrode materials.

graphite, which yielded concentrations of 55.9, 26.9, 18.9, and 9.6 mg L^{-1}, respectively. These findings clearly indicate that the novel OF-3D PyrC electrode is significantly more effective for direct microbial electrosynthesis of H_2O_2 via $2e^-$ ORR compared to pristine 3D PyrC electrodes and traditional 2D electrodes.[13] The rapid H_2O_2 synthesis observed using the OF-3D PyrC electrode is primarily attributed to the significant decrease in hydrophilicity of the modified electrode surface, which in turn increases the concentration of oxygen molecules at the electrode interface, enhancing their retention and reducing water accumulation, thereby promoting the efficiency of the two-electron ORR.[28]

In addition, previous studies on the MET found that anodic microorganisms have a significant impact on system performance.[14] Therefore, the corresponding control experiments (open circuit and abiotic cathode) were carried out, and the results showed that without anodic microorganisms, no H_2O_2 synthesis was detected. This difference may be due to the absence of anode microorganisms that harvest energy from substrate oxidation and transfer electrons to the anode, resulting in no current flowing in the system and halting of the H_2O_2 synthesis.

The findings indicate that the novel OF-3D PyrC electrode coupled with the MES reactor can reliably provide sustainable and highly effective on-site H_2O_2 production.

3.3. Influence of Operational Factors on Microbial Electrosynthesis of H_2O_2

3.3.1. Input Voltage. Although MES is acknowledged as an environmentally sustainable electrochemical device that harnesses electrical energy from wastewater, its energy utilization remains significant due to the necessity for an externally applied input voltage (generally below 1.0 V) during prolonged operation in MEC mode. Furthermore, the quantity of H_2O_2 generated in MEC mode does not necessarily exhibit a direct correlation with the input voltage, as elevated voltages may inadvertently provoke side reactions that undermine the current efficiency of the system, resulting in H_2O_2 production equivalent to or even inferior to that attained at lower voltages. Consequently, the influence of input voltage on H_2O_2

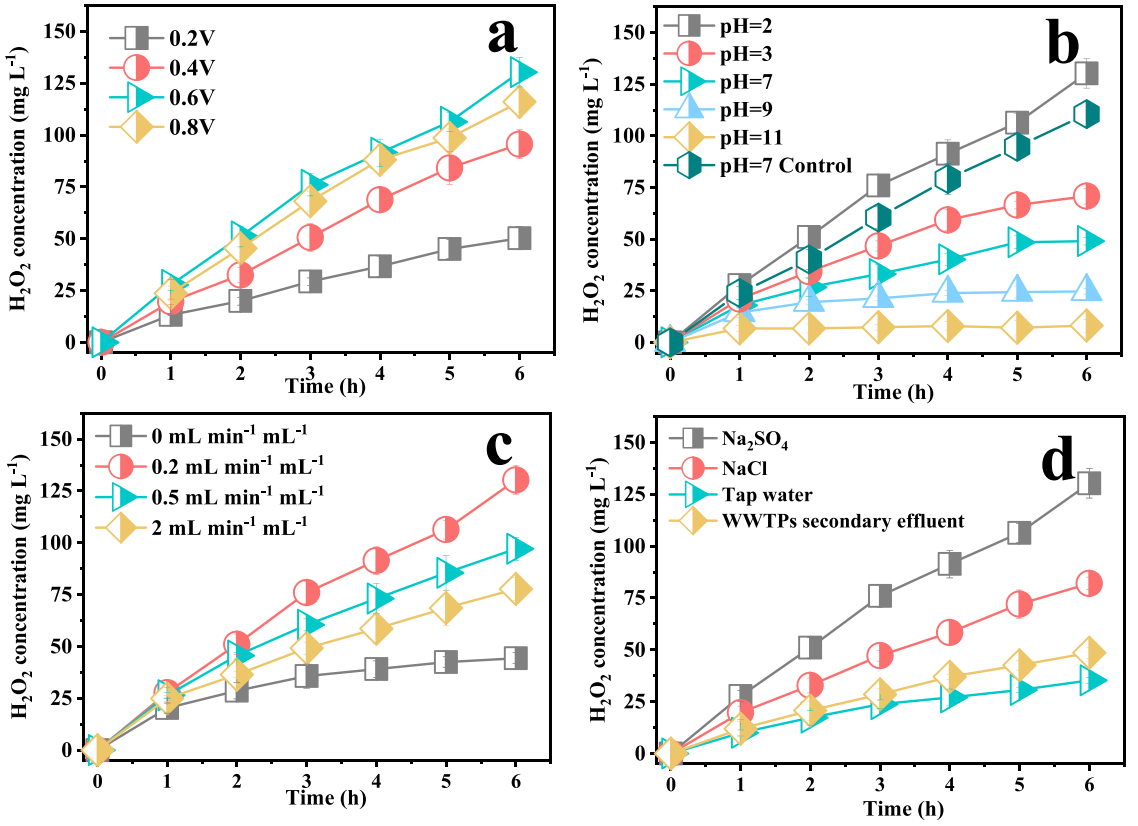

Figure 3. Effect of (a) input voltage, (b) pH, (c) cathodic aeration rate, and (d) catholyte type, on H_2O_2 production in a dual-chamber MES reactor using an OF-3D PyrC electrode.

https://doi.org/10.1021/acsenvironau.4c00067
ACS Environ. Au 2024, 4, 344−353

generation was investigated. The capability of the system for synthesizing H_2O_2 was assessed utilizing four voltages (0.2, 0.4, 0.6, and 0.8 V). Other operational parameters included an initial catholyte of 50 mM Na_2SO_4, pH 2, and an aeration velocity of 0.2 mL min^{-1} mL^{-1}.

Figure 3a illustrates that the concentration of H_2O_2 increased steadily over a 6 h period, with cumulative H_2O_2 concentrations of 50.2, 95.6, 130.2, and 116.1 mg L^{-1} for input voltages ranging from 0.2 to 0.8 V, respectively. Similar patterns were observed, showing an initial rise followed by a decrease in the accumulated H_2O_2 at the cathode as the voltage was raised when graphite was employed as the cathode material.[29,30] Initially, elevating the voltage from 0 to 0.6 V raises the current, which in turn enhances the charge transfer at the cathode. This improvement facilitates the cathodic two-electron ORR process to produce H_2O_2 (eq 1).[16,20,21] However, elevated currents may also initiate various side reactions as represented in eq 2), (3), (5) and (6)[9,31]

$$2H_2O_2 \rightarrow O_2 + 2H_2O \quad (5)$$

$$2H^+ + 2e^- \rightarrow H_2 \quad (6)$$

3.3.2. Initial Catholyte pH. It has been documented that pH influences the two-electron ORR kinetics at carbon-based electrodes, thus affecting H_2O_2 synthesis.[2] In this section, initial cathodic pH values of 2, 3, 7, 9, and 11 were selected to examine their effects on H_2O_2 generation. Other parameters included a starting electrolyte concentration of 50 mM Na_2SO_4, a voltage of 0.6 V, and an aeration velocity of 0.2 mL min^{-1} mL^{-1}.

As depicted in Figure 3b, the initial pH greatly affected the efficiency of cathodic microbial electrosynthesis of H_2O_2, with cumulative concentrations of 130.2, 70.8, 50.0, 24.7, and 8.1 mg L^{-1} over 6 h. Acidic conditions (pH 2) were clearly favorable for producing more H_2O_2. Notably, when the initial pH was 3 or higher, H_2O_2 accumulation in the cathode chamber initially increased but then declined. This occurrence is mainly due to the following reasons: In acidic electrolytes, the ORR prefers the two-electron pathway, whereas at elevated pH levels, hydrogenation is obstructed, and the four-electron ORR becomes predominant.[32] As shown in Figure 3b, the H_2O_2 concentration started to decline after the electrolyte reached alkaline conditions for initial pH levels of 3−9 (Figure S2). Additionally, the efficacy of the electrode in H_2O_2 synthesis under neutral conditions was assessed by maintaining the cathodic electrolyte at pH 7, as shown in Figure 3b. After 6 h, the accumulated H_2O_2 reached about 110.6 mg L^{-1}, comparable to the concentration at an initial pH of 2 and markedly higher than at other pH levels. These results demonstrate that the OF-3D PyrC electrode can efficiently produce H_2O_2 under both acidic and neutral conditions.

3.3.3. Cathodic Aeration Rate. Apart from voltage and pH, DO is pivotal for H_2O_2 synthesis at the 3D PyrC electrode, as indicated by eq 1. Typically, electrochemical production of H_2O_2 depends on substantial aeration rates (using air or pure O_2) to maintain an oxygen-rich solution, ensuring optimal H_2O_2 yield.[33] However, excessive aeration, which maintains or exceeds DO saturation in the catholyte, tends to decrease H_2O_2 production while escalating energy consumption. The ideal aeration rate optimizes H_2O_2 generation and minimizes expenses. Consequently, aeration rates ranging from 0 to 2 mL min^{-1} mL^{-1} were chosen to investigate their influence on H_2O_2 production.

As depicted in Figure 3c, after 6 h, the accumulated H_2O_2 concentrations were 44.3, 130.2, 97.1, and 77.7 mg L^{-1} for aeration rates of 0, 0.2, 0.5, and 2 mL min^{-1} mL^{-1}, respectively. Clearly, cathodic aeration significantly boosts H_2O_2 production compared to no aeration. The suboptimal system performance without aeration is due to an unsaturated catholyte, whereas it becomes saturated or supersaturated when the aeration rate reaches or exceeds 0.2 mL min^{-1} mL^{-1}, leading to enhanced mass transfer.[34] Additionally, the system currents recorded under aeration conditions are markedly higher than those without aeration (Figure S3), further corroborating the enhancement of mass transfer with aeration. Several factors may explain the negative effects of increasing the aeration rate from 0.2 to 2 mL min^{-1} mL^{-1}. Firstly, higher aeration rates generate more and larger bubbles, which increase the internal system resistance and reduce H_2O_2 production.[35−37] Secondly, increased aeration can disrupt the mass transfer between the catholyte and electrode, thereby decreasing the efficiency of the two-electron ORR.[38] These results highlight the importance of regulating cathodic aeration in MES with an OF-3D PyrC electrode for optimal H_2O_2 synthesis.

3.3.4. Catholyte Type. Due to the low conductivity of water, the electrosynthesis of H_2O_2 requires supporting electrolytes enhancing current flow and ensuring effective synthesis. Therefore, we examined the effects of common salts, including Na_2SO_4 and NaCl, as electrolytes on the microbial electrosynthesis of H_2O_2 using the innovative OF-3D PyrC electrode. Figure 3d shows that the type of catholyte significantly impacted H_2O_2 accumulation, with concentrations of 129.2 and 82.0 mg L^{-1} for Na_2SO_4 and NaCl, respectively. This indicates that Na_2SO_4 is the most favorable electrolyte for H_2O_2 production. The poorer performance with the other electrolytes (e.g., NaCl and $NaNO_3$) can be attributed to undesirable interactions between the electrolyte ions and the synthesized H_2O_2.[10,39] In the case of NaCl, Cl^- can react with the produced H_2O_2 in an acidic environment, as shown in eqs 7−11.[40]

$$H_2O_2 + 2H^+ + 2Cl^- \rightarrow Cl_2 + 2H_2O \quad (7)$$

$$H_2O_2 + H^+ + Cl^- \rightarrow ClO^- + H_2O \quad (8)$$

$$H_2O_2 + ClO^- \rightarrow Cl^- + O_2 + H_2O \quad (9)$$

$$ClO^- \rightarrow {}^{\bullet}O^- + {}^{\bullet}Cl \quad (10)$$

$${}^{\bullet}Cl + H_2O_2 \rightarrow {}^{\bullet}HO_2 + H^+ + Cl^- \quad (11)$$

The dosage of supporting electrolytes impacts operational expenses, and the production of H_2O_2 with elevated concentrations of electrolytes will also raise future purification costs. In consequence, we further evaluated the influence of employing tap water and WWTPs secondary effluent as cathodic electrolytes on H_2O_2 production performance. As depicted in Figure 3d, the accumulated H_2O_2 exhibited a dramatic decline from 130.2 mg L^{-1} to 35.2 and 48.6 mg L^{-1}, primarily attributable to the lower conductivity of tap water and WWTPs secondary effluent. Nevertheless, given that the H_2O_2 concentration remains close to 50 mg L^{-1}, it satisfies the requirements for H_2O_2 dosage in H_2O_2-mediated water treatment processes (e.g., Fenton processes), which typically range from 10 to 50 mg L^{-1}.[13] The utilization of the OF-3D PyrC electrode facilitates high yields of H_2O_2 without necessitating additional supporting electrolytes, thereby

https://doi.org/10.1021/acsenvironau.4c00067
ACS Environ. Au 2024, 4, 344−353

enhancing the cost-effectiveness of subsequent water treatment processes that leverage this generated H_2O_2.

3.4. Electrochemical Stability Tests, Energy Consumption and Cost of OF-3D PyrC Electrode for Repeated Electrosynthesis of H_2O_2

Assessing the durability of the OF-3D PyrC electrode fabricated using additive manufacturing techniques is crucial for its potential future applications. Consequently, the performance of microbial electrosynthesis of H_2O_2 was evaluated over 10 consecutive cycles of the MES utilizing this electrode. The experimental conditions were maintained according to previously established optimal operating parameters, with the sole alteration being the replacement of the catholyte at the conclusion of each cycle. As illustrated in Figure 4a, the H_2O_2 accumulation at the cathode after 10

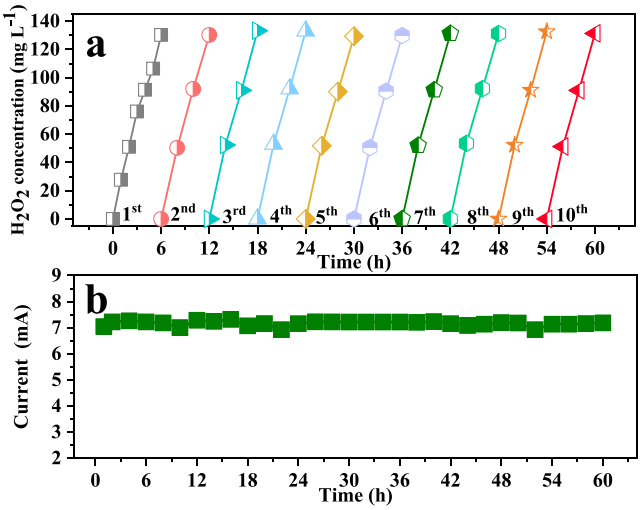

Figure 4. Evaluation of the reusability of OF-3D PyrC electrode in a dual-chamber MES reactor. (a) H_2O_2 production and (b) recorded system current for 10 consecutive cycles.

consecutive cycles remained virtually unchanged, with a concentration of approximately 131 mg L^{-1}, indicating that the electrode experienced no deactivation. Throughout this period, the system current consistently maintained a value of 7.2 mA over the 10 cycles (Figure 4b). These results indicate that the innovative OF-3D PyrC electrode exhibits remarkable stability and reproducibility for microbial electrochemical H_2O_2 production.

The principal operational expenditure of the MES for H_2O_2 synthesis is attributed to the electrical energy consumption (direct current power supply input, stirring, and aeration) of the process. For the OF-3D PyrC electrode, the computed electrical energy consumption was 0.6 kWh kg^{-1} H_2O_2, as derived from the formula detailed in Text S3. Moreover, energy consumption data from prior research on MES for H_2O_2 synthesis using various cathode materials are summarized in Table S2. The OF-3D PyrC electrode demonstrates markedly lower energy consumption compared to traditional 2D electrodes in MES (1.1 to 99.6 kWh kg^{-1} H_2O_2). Table S2 also highlights that a 3D graphite particle electrode, comprising PTFE-modified graphite particles (2−3 mm) manufactured via nonadditive manufacturing methods, achieved a superior H_2O_2 production rate (88.2 vs 21.7 mg L^{-1} h^{-1}) compared to the OF-3D PyrC electrode. This enhancement is due to the effective direct oxygen uptake by the electrode's porous structure, facilitated by PTFE modification, which addresses the issue of low oxygen solubility. Nevertheless, the inclusion of the PTFE catalytic layer raises costs and presents challenges regarding long-term performance. Furthermore, it has been shown that the E/EO value can be minimized when increasing the processing capacity from laboratory scale (2.2 kWh m^{-3}) to pilot scale (0.68 kWh m^{-3}) or even full scale (0.5 kWh m^{-3}) during the UV/H_2O_2 process.[41] Similarly, the use of the novel OF-3D PyrC electrode for H_2O_2 synthesis in MES reactors is expected to further decrease energy consumption as the reactor scale increases, making the process even more energy-efficient and competitive for practical applications.

In our current lab-scale setup, the cost of producing a pristine 3D PyrC electrode is roughly 5 USD. The additional cost to fabricate the OF-3D PyrC electrode is minimal, with the price difference between the two types of electrodes being less than 1 USD. This estimate accounts for both material costs and the energy required for the 3D printing and pyrolysis processes. It is important to highlight that this cost estimate reflects our small-scale, manual production methods, which involve limited batch sizes. If scaled up to mass production, where more efficient and automated techniques are employed, the costs could be significantly reduced. Our fabrication process shows strong potential for creating high-performance electrodes at an affordable price. We believe that with further optimization, we can lower production costs even further and pave the way for the commercialization of our technology.

3.5. Feasibility and Applicability in a BEF Process for Effective Removal of Pharmaceuticals and Eco-toxicity Test

The OF-3D PyrC electrodes in the MES effectively generate H_2O_2 at acidic pH (e.g., pH 2), optimal for the Fenton process. Thus, we explored this innovative electrode in the BEF field as a tertiary treatment for removing refractory micropollutants from secondary effluent in WWTPs. We tested the removal of 24 pharmaceuticals spiked in real secondary effluent from Lyngby WWTP in Copenhagen, Denmark, as detailed in Table S1. The results illustrated in Figure 5 demonstrate that the removal of the selected 24 typical pharmaceuticals adheres to first-order kinetics, exhibiting substantial variability in removal rates, yet all were completely eliminated within 3 h. Remarkably, 16 of these pharmaceuticals (azithromycin, atenolol, bezafibrate, carbamazepine, clarithromycin, chlorpheniramine, diclofenac, hydrochlorothiazide, iohexol, propranolol, metoprolol, mefenamic acid, mycophenolic acid, sertraline, sulfamethoxazole, and venlafaxine) were eradicated in 1 h or less. Moreover, the BEF process utilizing the OF-free 3D PyrC electrode significantly surpassed the BEF process with the pristine 3D PyrC electrode, primarily attributable to the elevated H_2O_2 yield, which consequently resulted in a greater production of hydroxyl radicals ($^{\bullet}OH$) generated through eq 12.[13,30,42]

$$H_2O_2 + Fe^{2+} \rightarrow Fe^{3+} + {}^{\bullet}OH + OH^- \quad (12)$$

The safety of the BEF process with OF-3D PyrC electrodes as a tertiary treatment was assessed using *Vibrio fischeri* to evaluate the ecotoxicity of the effluent. Inhibition rates below 20% are generally considered to have no significant harmful effects.[13] Figure 6 shows that bioluminescence inhibition at the beginning of the treatment reached 57 and 72% for the toxicity assessment at assay times of 10 and 20 min, respectively, indicating initial biotoxicity due to 24 added pharmaceuticals,

https://doi.org/10.1021/acsenvironau.4c00067
ACS Environ. Au 2024, 4, 344−353

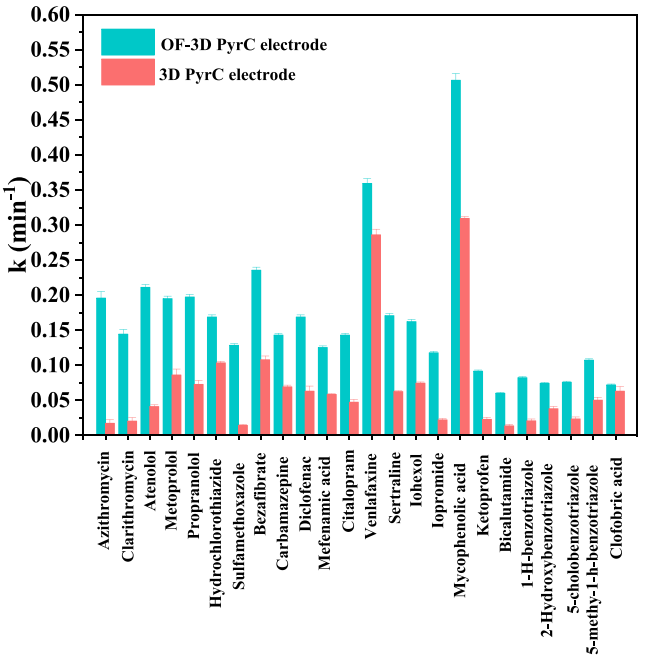

Figure 5. Pseudo-first-order rate constants (k) of the degradation of 24 typical pharmaceuticals from WWTP secondary effluent during BEF treatment using an OF-3D PyrC electrode and pristine 3D PyrC electrode.

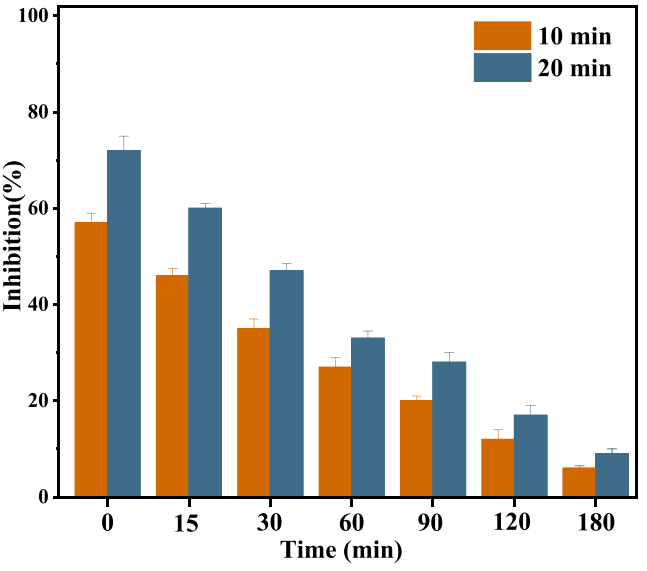

Figure 6. Toxicity assessment at two assay times of 10 and 20 min in terms of inhibition percentage of *Vibrio fischeri* for the BEF treated effluent using an OF-3D PyrC electrode.

including antibiotics. However, inhibition levels dropped below 20% after 2 h and below 10% after 3 h, demonstrating effective detoxification and confirming the BEF process as a safe, eco-friendly wastewater treatment method.

3.6. Environmental Implication

Recalcitrant micropollutants in wastewater present substantial threats to ecosystems and public health. H_2O_2 is a green oxidizing agent that has become increasingly important in diverse applications, especially in environmental remediation. This study unveils an innovative electrode design that combines state-of-the-art additive manufacturing with surface modification techniques, bioelectrochemistry, and Fenton processes. Compared to traditional 2D and pristine 3D PyrC electrodes, this OF-3D PyrC electrode offers the following advantages: (1) Efficient H_2O_2 synthesis: Effective and sustainable microbial production of H_2O_2 under acidic and neutral conditions, providing sufficient oxidants for water treatment. (2) Stability and durability: After 10 consecutive cycles, the cathodic synthesis of H_2O_2 remains nearly unchanged, demonstrating excellent stability. (3) Strong applicability: It is suitable for use in the BEF process, effectively removing various micropollutants, particularly the 24 representative pharmaceuticals commonly found in European water environments. Despite its promising potential, several challenges remain: (1) Electrode fabrication costs need to be further reduced; (2) Gas−liquid mass transfer efficiency needs to be further improved.

To address these challenges, targeted strategies can be implemented: (1) Reducing electrode fabrication costs by optimizing materials, using more affordable and sustainable alternatives, and streamlining the manufacturing process to enhance efficiency and lower unit costs. (2) Enhancing gas−liquid mass transfer efficiency through electrode structural optimization, incorporating advanced internal aeration techniques for better oxygen distribution, and designing high-efficiency flow reactors to improve mixing and contact between gas and liquid phases.

4. CONCLUSIONS

In this study, we developed a straightforward method for creating structured OF-3D PyrC electrodes using additive manufacturing, surface modification and pyrolysis. These electrodes were tested in a MES reactor to improve H_2O_2 synthesis, outperforming traditional carbon electrodes (e.g., graphite) and pristine 3D PyrC electrodes in cathodic H_2O_2 production due to less hydrophilicity. The electrodes achieved approximately 130.2 mg L^{-1} of H_2O_2 in 6 h under optimal conditions, with stable performance output across multiple cycles. This effective H_2O_2 production enhanced the removal of 24 typical pharmaceuticals in the subsequent BEF process. This method eliminates the need for expensive modifications such as incorporation of catalysts, making it more economical. Furthermore, the electrodes demonstrated excellent reusability, positioning them well for large-scale applications. This innovative approach offers a pathway for sustainable and cost-effective H_2O_2 synthesis, facilitating broader implementation of the BEF process.

■ ASSOCIATED CONTENT

Supporting Information

The Supporting Information is available free of charge at https://pubs.acs.org/doi/10.1021/acsenvironau.4c00067.

Chemicals and Reagents, detailed computational method and operating parameters of the HPLC-MS/MS system, main characteristics of WWTP secondary effluent, previous studies on (microbial) electrosynthesis of H_2O_2 using different types of cathode electrodes, schematic illustration of the BES reactor, and the effect of initial catholyte pH (catholyte pH variation) on H_2O_2 production in the MES reactor (PDF)

https://doi.org/10.1021/acsenvironau.4c00067
ACS Environ. Au 2024, 4, 344−353

AUTHOR INFORMATION

Corresponding Author

Yifeng Zhang − *Department of Environmental & Resource Engineering, Technical University of Denmark, DK-2800 Kgs. Lyngby, Denmark;* orcid.org/0000-0002-2832-2277; Phone: (+45) 45251410; Email: yifz@dtu.dk, yifzmfc@gmail.com; Fax: (+45) 45933850

Authors

Rusen Zou − *Department of Environmental & Resource Engineering, Technical University of Denmark, DK-2800 Kgs. Lyngby, Denmark*

Babak Rezaei − *National Centre for Nano Fabrication and Characterization, DTU Nanolab, Technical University of Denmark, DK-2800 Kgs. Lyngby, Denmark;* orcid.org/0000-0002-8177-5363

Stephan Sylvest Keller − *National Centre for Nano Fabrication and Characterization, DTU Nanolab, Technical University of Denmark, DK-2800 Kgs. Lyngby, Denmark;* orcid.org/0000-0003-4108-1305

Complete contact information is available at: https://pubs.acs.org/10.1021/acsenvironau.4c00067

Author Contributions

§R.Z. and B.R. contributed equally to this study.

Notes

The authors declare no competing financial interest.

ACKNOWLEDGMENTS

Y.Z. acknowledge the financial support from The Carlsberg Foundation (CF18-0084), VILLUM FONDEN (No.40828, Denmark), and Independent Research Fund Denmark (Project 1, No.171114, Denmark). B.R. and S.S.K. acknowledge the financial support from the European Research Council under the Horizon 2020 framework program (Grant No. 772370-PHOENEEX).

REFERENCES

(1) He, H.; Liu, S.; Liu, Y.; Zhou, L.; Wen, H.; Shen, R.; Zhang, H.; Guo, X.; Jiang, J.; Li, B. Review and Perspectives on Carbon-based Electrocatalysts for Production of H2O2 via Two-electron Oxygen Reduction *Green Chem.* 2023.

(2) Bu, Y.; Wang, Y.; Han, G. F.; Zhao, Y.; Ge, X.; Li, F.; Zhang, Z.; Zhong, Q.; Baek, J. B. Carbon-Based Electrocatalysts for Efficient Hydrogen Peroxide Production. *Adv. Mater.* **2021**, *33*, No. 2103266.

(3) Liu, X.-W.; Sun, X.-F.; Li, D.-B.; Li, W.-W.; Huang, Y.-X.; Sheng, G.-P.; Yu, H.-Q. Anodic Fenton process assisted by a microbial fuel cell for enhanced degradation of organic pollutants. *Water Res.* **2012**, *46* (14), 4371−4378.

(4) Campos-Martin, J. M.; Blanco-Brieva, G.; Fierro, J. L. Hydrogen peroxide synthesis: an outlook beyond the anthraquinone process. *Angew. Chem., Int. Ed.* **2006**, *45* (42), 6962−6984.

(5) Perry, S. C.; Pangotra, D.; Vieira, L.; Csepei, L.-I.; Sieber, V.; Wang, L.; Ponce de León, C.; Walsh, F. C. Electrochemical synthesis of hydrogen peroxide from water and oxygen. *Nat. Rev. Chem.* **2019**, *3* (7), 442−458.

(6) Jiang, Y.; Ni, P.; Chen, C.; Lu, Y.; Yang, P.; Kong, B.; Fisher, A.; Wang, X. Selective electrochemical H_2O_2 production through two-electron oxygen electrochemistry. *Adv. Energy Mater.* **2018**, *8* (31), No. 1801909.

(7) Fan, W.; Zhang, B.; Wang, X.; Ma, W.; Li, D.; Wang, Z.; Dupuis, M.; Shi, J.; Liao, S.; Li, C. Efficient hydrogen peroxide synthesis by metal-free polyterthiophene via photoelectrocatalytic dioxygen reduction. *Energy Environ. Sci.* **2020**, *13* (1), 238−245.

(8) Sun, Y.; Sinev, I.; Ju, W.; Bergmann, A.; Dresp, S.; Kuhl, S.; Spori, C.; Schmies, H.; Wang, H.; Bernsmeier, D.; et al. Efficient electrochemical hydrogen peroxide production from molecular oxygen on nitrogen-doped mesoporous carbon catalysts. *ACS Catal.* **2018**, *8* (4), 2844−2856.

(9) Wang, W.; Lu, X.; Su, P.; Li, Y.; Cai, J.; Zhang, Q.; Zhou, M.; Arotiba, O. Enhancement of hydrogen peroxide production by electrochemical reduction of oxygen on carbon nanotubes modified with fluorine. *Chemosphere* **2020**, *259*, No. 127423.

(10) Zou, R.; Hasanzadeh, A.; Khataee, A.; Yang, X.; Xu, M.; Angelidaki, I.; Zhang, Y. Scaling-up of microbial electrosynthesis with multiple electrodes for in situ production of hydrogen peroxide *IScience* 2021; Vol. *24* 2 DOI: 10.1016/j.isci.2021.102094.

(11) Chung, T. H.; Dhar, B. R. A mini-review on applications of 3D printing for microbial electrochemical technologies. *Front. Energy Res.* **2021**, *9*, No. 679061.

(12) Theodosiou, P.; Greenman, J.; Ieropoulos, I. A. Developing 3D-printable cathode electrode for monolithically printed microbial fuel cells (MFCs). *Molecules* **2020**, *25* (16), 3635.

(13) Zou, R.; Rezaei, B.; Keller, S. S.; Zhang, Y. Additive manufacturing-derived free-standing 3D pyrolytic carbon electrodes for sustainable microbial electrochemical production of H_2O_2. *J. Hazard Mater.* **2024**, *467*, No. 133681.

(14) Li, X.; Chen, S.; Angelidaki, I.; Zhang, Y. Bio-electro-Fenton processes for wastewater treatment: Advances and prospects. *Chem. Eng. J.* **2018**, *354*, 492−506.

(15) Chung, T. H.; Meshref, M. N.; Hai, F. I.; Al-Mamun, A.; Dhar, B. R. Microbial electrochemical systems for hydrogen peroxide synthesis: Critical review of process optimization, prospective environmental applications, and challenges. *Bioresour. Technol.* **2020**, *313*, No. 123727.

(16) Yu, F.; Zhou, M.; Yu, X. Cost-effective electro-Fenton using modified graphite felt that dramatically enhanced on H_2O_2 electro-generation without external aeration. *Electrochim. Acta* **2015**, *163*, 182−189.

(17) Rezaei, B.; Pan, J. Y.; Gundlach, C.; Keller, S. S. Highly structured 3D pyrolytic carbon electrodes derived from additive manufacturing technology. *Mater. Design* **2020**, *193*, No. 108834.

(18) Sun, Q.; Dolle, C.; Kurpiers, C.; Kraft, K.; Islam, M.; Schwaiger, R.; Gumbsch, P.; Eggeler, Y. M. In Situ Pyrolysis of 3D Printed Building Blocks for Functional Nanoscale Metamaterials. *Adv. Funct. Mater.* **2024**, *34* (20), No. 2302358.

(19) Eggeler, Y. M.; Chan, K. C.; Sun, Q.; Lantada, A. D.; Mager, D.; Schwaiger, R.; Gumbsch, P.; Schröder, R.; Wenzel, W.; Korvink, J. G.; Islam, M. A review on 3D architected pyrolytic carbon produced by additive micro/nanomanufacturing. *Adv. Funct. Mater.* **2024**, *34* (20), No. 2302068.

(20) Rezaei, B.; Hansen, T. W.; Keller, S. S. Stereolithography-derived three-dimensional pyrolytic carbon/Mn_3O_4 nanostructures for free-standing hybrid supercapacitor electrodes. *ACS Appl. Nano Mater.* **2022**, *5* (2), 1808−1819.

(21) Lu, Z.; Chen, G.; Siahrostami, S.; Chen, Z.; Liu, K.; Xie, J.; Liao, L.; Wu, T.; Lin, D.; Liu, Y.; et al. High-efficiency oxygen reduction to hydrogen peroxide catalysed by oxidized carbon materials. *Nat. Catal.* **2018**, *1* (2), 156−162.

(22) Ren, X.; Dong, X.; Liu, L.; Hao, J.; Zhu, H.; Liu, A.; Wu, G. Research progress of electrocatalysts for the preparation of H_2O_2 by electrocatalytic oxygen reduction reaction. *SusMat* **2023**, *3* (4), 442−470.

(23) van der Heijden, M.; Kroese, M.; Borneman, Z.; Forner-Cuenca, A. Investigating mass transfer relationships in stereolithography 3D printed electrodes for redox flow batteries. *Adv. Mater. Technol.* **2023**, *8* (18), No. 2300611.

(24) Pan, J. Y.; Rezaei, B.; Anhøj, T. A.; Larsen, N. B.; Keller, S. S. Hybrid microfabrication of 3D pyrolytic carbon electrodes by photolithography and additive manufacturing. *Micro Nano Eng.* **2022**, *15*, No. 100124.

(25) Xie, Q.; Chen, G.; Bao, R.; Zhang, Y.; Wu, S. Polystyrene foam derived nitrogen-enriched porous carbon/graphene composites with high volumetric capacitances for aqueous supercapacitors. *Micropor. Mesopor. Mater.* **2017**, *239*, 130−137.
(26) Maitra, T.; Sharma, S.; Srivastava, A.; Cho, Y.-K.; Madou, M.; Sharma, A. Improved graphitization and electrical conductivity of suspended carbon nanofibers derived from carbon nanotube/polyacrylonitrile composites by directed electrospinning. *Carbon* **2012**, *50* (5), 1753−1761.
(27) Yu, X.; Zhou, M.; Ren, G.; Ma, L. A novel dual gas diffusion electrodes system for efficient hydrogen peroxide generation used in electro-Fenton. *Chem. Eng. J.* **2015**, *263*, 92−100.
(28) He, Y.; Liu, S.; Priest, C.; Shi, Q.; Wu, G. Atomically dispersed metal−nitrogen−carbon catalysts for fuel cells: advances in catalyst design, electrode performance, and durability improvement. *Chem. Soc. Rev.* **2020**, *49* (11), 3484−3524.
(29) Zou, R.; Tang, K.; Angelidaki, I.; Andersen, H. R.; Zhang, Y. An innovative microbial electrochemical ultraviolet photolysis cell (MEUC) for efficient degradation of carbamazepine. *Water Res.* **2020**, *187*, No. 116451.
(30) Zou, R.; Angelidaki, I.; Yang, X.; Tang, K.; Andersen, H. R.; Zhang, Y. Degradation of pharmaceuticals from wastewater in a 20-L continuous flow bio-electro-Fenton (BEF) system. *Sci. Total Environ.* **2020**, *727*, No. 138684.
(31) Chen, J.-y.; Zhao, L.; Li, N.; Liu, H. A microbial fuel cell with the three-dimensional electrode applied an external voltage for synthesis of hydrogen peroxide from organic matter. *J. Power Sources* **2015**, *287*, 291−296.
(32) Chai, G.-L.; Hou, Z.; Ikeda, T.; Terakura, K. Two-electron oxygen reduction on carbon materials catalysts: mechanisms and active sites. *J. Phys. Chem. C* **2017**, *121* (27), 14524−14533.
(33) Moreira, F. C.; Boaventura, R. A.; Brillas, E.; Vilar, V. J. Electrochemical advanced oxidation processes: a review on their application to synthetic and real wastewaters. *Appl. Catal. B-Environ.* **2017**, *202*, 217−261.
(34) Sim, J.; An, J.; Elbeshbishy, E.; Ryu, H.; Lee, H.-S. Characterization and optimization of cathodic conditions for H_2O_2 synthesis in microbial electrochemical cells. *Bioresour. Technol.* **2015**, *195*, 31−36.
(35) Salmerón, I.; Plakas, K. V.; Sirés, I.; Oller, I.; Maldonado, M. I.; Karabelas, A. J.; Malato, S. Optimization of electrocatalytic H_2O_2 production at pilot plant scale for solar-assisted water treatment. *Appl. Catal. B-Environ.* **2019**, *242*, 327−336.
(36) Freakley, S. J.; Piccinini, M.; Edwards, J. K.; Ntainjua, E. N.; Moulijn, J. A.; Hutchings, G. J. Effect of reaction conditions on the direct synthesis of hydrogen peroxide with a AuPd/TiO_2 catalyst in a flow reactor. *ACS Catal.* **2013**, *3* (4), 487−501.
(37) Nadais, H.; Li, X.; Alves, N.; Couras, C.; Andersen, H. R.; Angelidaki, I.; Zhang, Y. Bio-electro-Fenton process for the degradation of Non-Steroidal Anti-Inflammatory Drugs in wastewater. *Chem. Eng. J.* **2018**, *338*, 401−410.
(38) Li, X.; Angelidaki, I.; Zhang, Y. Salinity-gradient energy driven microbial electrosynthesis of hydrogen peroxide. *J. Power Sources* **2017**, *341*, 357−365.
(39) Zou, R.; Rezaei, B.; Yang, X.; Zhang, W.; Keller, S. S.; Zhang, Y. Novel bio-solar hybrid photoelectrochemical synthesis for selective hydrogen peroxide production *Green Chem.* 2024; Vol. *26* DOI: 10.1039/D4GC02220C.
(40) Lai, X.; Ning, X.-a.; Chen, J.; Li, Y.; Zhang, Y.; Yuan, Y. Comparison of the Fe^{2+}/H_2O_2 and Fe^{2+}/PMS systems in simulated sludge: Removal of PAHs, migration of elements and formation of chlorination by-products. *J. Hazard Mater.* **2020**, *398*, No. 122826.
(41) Miklos, D. B.; Remy, C.; Jekel, M.; Linden, K. G.; Drewes, J. E.; Hübner, U. Evaluation of advanced oxidation processes for water and wastewater treatment−A critical review. *Water Res.* **2018**, *139*, 118−131.
(42) Wang, G.; Yao, Y.; Tang, K.; Wang, G.; Zhang, W.; Zhang, Y.; Andersen, H. R. Cost-efficient microbial electrosynthesis of hydrogen peroxide on a facile-prepared floating electrode by entrapping oxygen. *Bioresour. Technol.* **2021**, *342*, No. 125995.

https://doi.org/10.1021/acsenvironau.4c00067
ACS Environ. Au 2024, 4, 344−353